Protoplasma (1994) 181: 106–122

PROTOPLASMA

Structure and development of the cryptomonad periplast: a review

S. J. Brett, L. Perasso[+], and R. Wetherbee***

School of Botany, University of Melbourne, Parkville, Victoria

Received March 30, 1994
Accepted April 30, 1994

Summary. The structure and development of the complex periplast, or cell covering, of cryptomonads is reviewed. The periplast consists of the plasma membrane (PM) plus an associated surface periplast component (SPC) and cytoplasmic or inner periplast component (IPC). The structure of the SPC and IPC, and their association with the PM, varies considerably between genera. This review, which concentrates on cryptomonads with an IPC of discrete plates, discusses relationships between periplast components and examines the development of this unique cell covering. Formation and growth of inner plates occurs throughout the cell cycle from specialized regions termed anamorphic zones. Crystalline surface plates, which comprise the SPC in many cryptomonad species, appear to form by self-assembly of disorganized subunits. In *Komma caudata* the subunits are composed of a high molecular weight glycoprotein that is produced within the endomembrane system and deposited onto the cell surface within anamorphic zones. The self-assembly of subunits into highly ordered surface plates appears closely associated with developmental changes in the underlying IPC and PM.

Keywords: Cryptophyceae; Cell wall; Periplast; Self-assembly; Freeze fracture-freeze etch.

Introduction

The cryptomonads are a unique group of phytoflagellates, easily distinguished from other microalgae by their asymmetric shape. The distinctive appearance of these cells can be attributed, in part, to the possession of a subapical depression (termed the vestibulum) which may extend internally to form a gullet (Santore 1987; Hill and Wetherbee 1990; Hill 1991 a, b) or progress along the ventral surface into a furrow (Munawar and Bistricki 1979, Klaveness 1981, 1985, Kugrens et al. 1986). The vestibulum/furrow/gullet complex forms an important surface feature of all cryptomonad cells, and three major categories may be recognized within the group (Kugrens and Lee 1991) (Fig. 1).

The characteristic shape of the cryptomonads is maintained by a complex structure termed the periplast, which is present across most peripheral regions of the cell but never extends into the vestibulum, furrow or

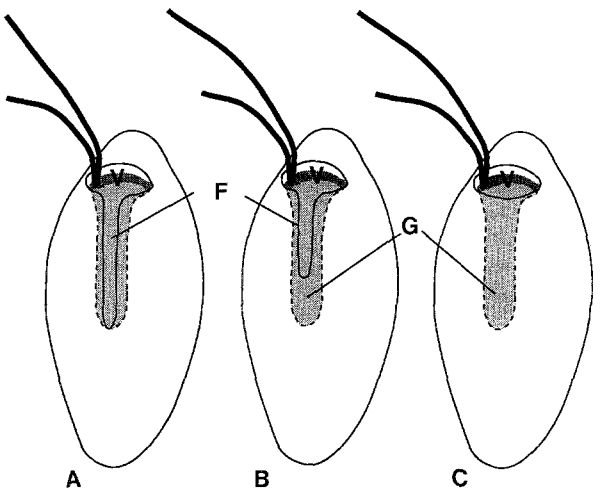

Fig. 1 A–C. Organization of the vestibulum (*V*), furrow (*F*), and gullet (*G*) in the Cryptophyceae. **A** In *Proteomonas, Falcomonas, Plagioselmis*, and *Teleaulax* a furrow progresses along the ventral surface from the vestibulum. **B** *Rhodomonas, Cryptomonas, Capylomonas*, and *Geminigera* possess both furrow and gullet. **C** The vestibulum extends internally to form a gullet in *Komma, Chroomonas, Rhinomonas, Hemiselmis, Guillardia*, and *Storeatula*

* Correspondence and reprints: School of Botany, University of Melbourne, Parkville, Vic 3052, Australia.
** Present address: Bigelow Laboratory for Ocean Sciences, W. Boothbay Harbor, Maine, U.S.A.
[+] Present address: Botanisches Institut, Universität zu Köln, Federal Republic of Germany.

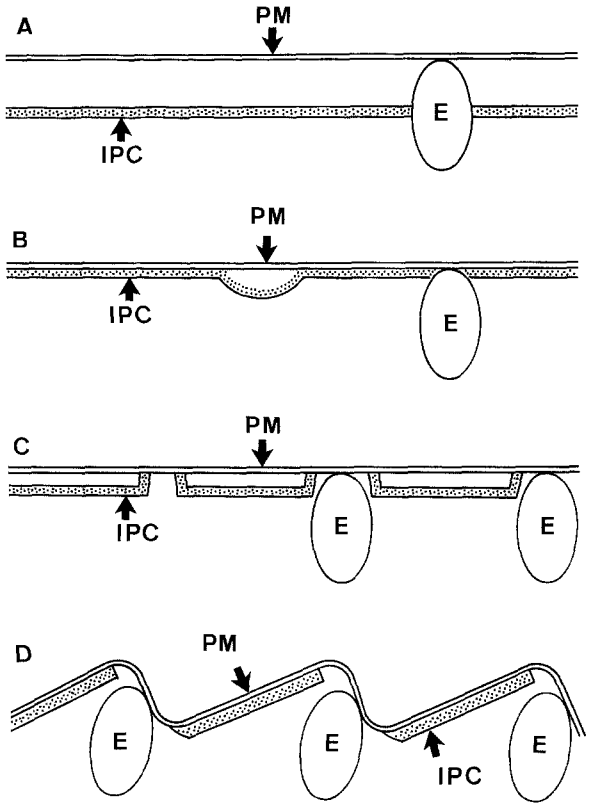

Fig. 2 A–D. Variations in inner periplast component (ICP) morphology throughout the Cryptophyceae. **A** ICP comprising a continuous sheet of material which is never closely associated with the PM. Ejectisomes (*E*) pass through pores in this sheet to contact the PM. **B** IPC comprising continuous sheet of material, closely appressed to the PM. This sheet may occasionally appear separated from the PM. **C** IPC consisting of discrete plates which are strongly attached to the PM at their edges. **D** IPC of discrete anteriorly stepped plates closely appressed to the PM. Ejectisome vesicles associate with PM adjacent to the anterior corners of plates

gullet. The morphology of this organelle differs markedly from the cell wall or cytoskeletal structures of other phytoflagellates. The general organization is similar in all cryptomonads, with the periplast consisting of an inner periplast component (IPC) and an additional surface periplast component (SPC) that support cells via a close association with the plasma membrane (PM) (Dodge 1969, Lucas 1970, Gantt 1971, Hibberd et al. 1971, Faust 1974, Santore 1977). Digestion of both the IPC and SPC using trypsin in several early EM studies (Gantt 1971, Faust 1974) led to the suggestion that the periplast components may be proteinaceous, while a more recent investigation of the composition of the SPC in a single species revealed a high molecular weight glycoprotein (Perasso et al. in prep.).

Examination of cryptomonad cells using scanning electron microscopy (SEM), thin sections and, more recently, freeze-fracture and freeze-etch has enabled accurate determination of periplast morphology in a wide range of genera. Studies incorporating these techniques reveal considerable variation in structure and organization of the IPC and SPC throughout the Cryptophyceae.

The IPC, which appears to form the primary structural elements of the periplast in all cryptomonads, may consist of a continuous sheet of material situated beneath the PM (Grim and Stahelin 1984; Brett and Wetherbee 1986; Hill and Wetherbee 1986; Wetherbee et al. 1986, 1987) or comprise a highly ordered system of discrete internal plates (Gantt 1971; Faust 1974; Hausmann and Walz 1979; Hill and Wetherbee 1986, 1988, 1989; Kugrens and Lee 1987). These differences, and further variations in the relationship between IPC and PM, enable recognition of four major IPC types within the group (Fig. 2).

Morphology of the SPC also varies markedly between taxa. Although early workers recognized some differences in surface organization from thin sectioned material (e.g., Santore 1977), detailed examination of the SPC was not possible until the incorporation of freeze-etch into the methodology. Use of this technique has allowed investigation of surface microarchitecture, revealing that the SPC may range from dense mats of fibrillar material (Fig. 3) to complex rosulate scales (Fig. 4) or highly ordered surface plates (Fig. 5) (Brett and Wetherbee 1986; Wetherbee et al. 1986, 1987; Hill and Wetherbee 1986, 1988, 1989, 1990).

In addition to enabling investigation of the gross details of periplast morphology, use of a combination of EM techniques (in particular freeze-fracture and freeze-etch) has revealed an extremely close relationship between the IPC, PM and SPC in many cryptomonads. Although the association between these periplast components has now been investigated in a wide range of genera (e.g., Hausmann and Walz 1979; Wetherbee et al. 1986, 1987; Kugrens and Lee 1987; Hill 1991 a, b), this review will concentrate on cells with an IPC composed of discrete internal plates. These cryptomonads, which include members of eight distinct genera (Table 1), provide model systems for examination of the interaction between IPC, PM and SPC and have been used extensively to investigate the mode of development of this unique and complex organelle (Brett and Wetherbee in prep.; Perasso et al. in prep.).

The inner periplast component and the plasma membrane

The plates that comprise the IPC in many cryptomonads often display some variation in shape and orga-

nization between genera. Details of the IPC, examined directly using thin sections and indirectly in freeze-fracture images, show two major types of inner plate within the group, and reveal differences within each of these types (Table 1). In most genera the inner plates are arranged into offset longitudinal rows which pass from the vestibular margins toward the cell posterior (Gantt 1971; Hill and Wetherbee 1986, 1988, 1989; Hill 1991 b). These plates are closely appressed to the underside of the PM and are anteriorly stepped, giving the periplast a serrated appearance in thin-sections (Fig. 6). Membrane-bound extrusive organelles (termed ejectisomes) are normally positioned adjacent to the anterior corners of each plate, and associate with the

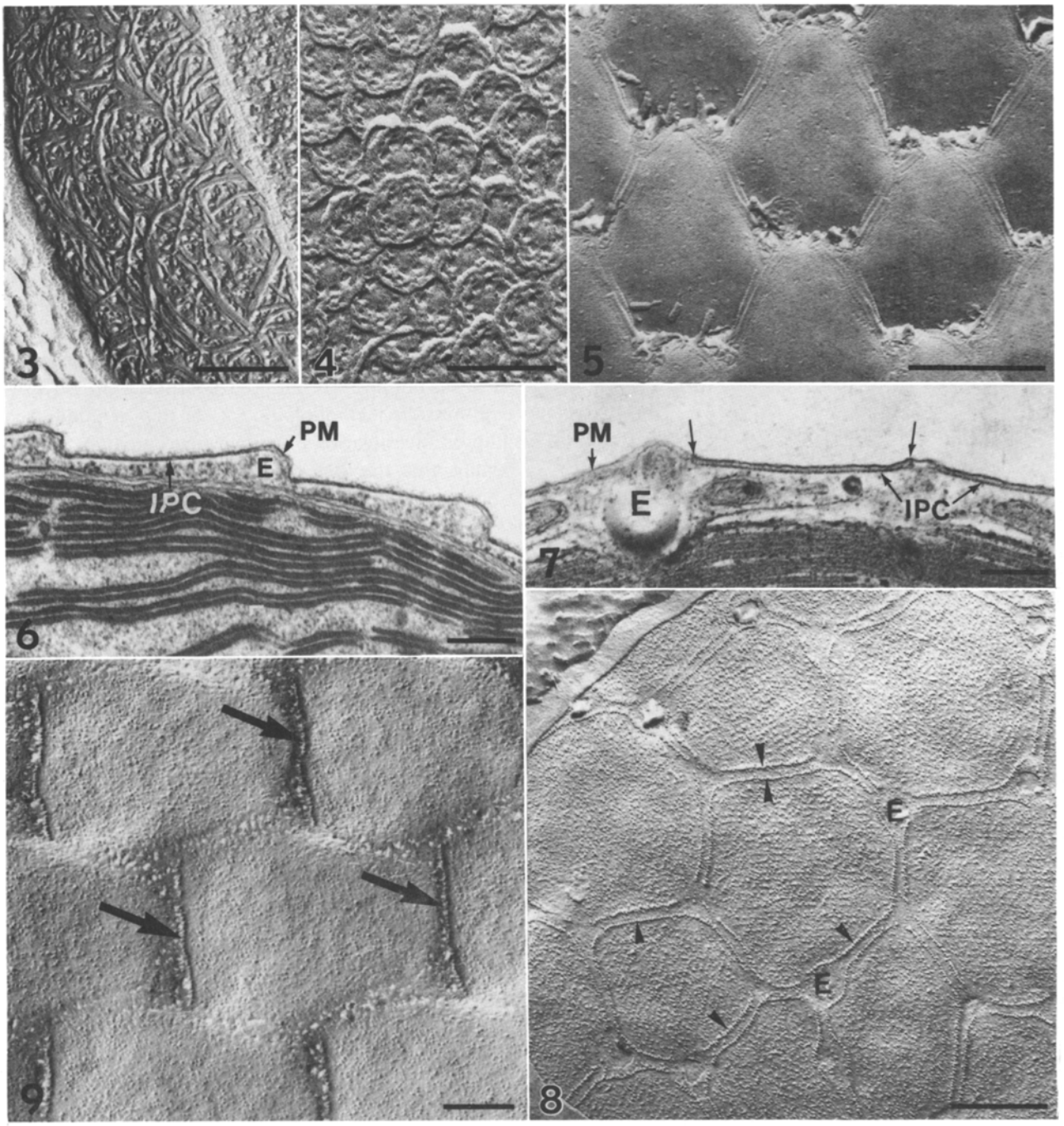

PM in these regions (Antia et al. 1973; Santore 1977, 1982, 1986, 1987; Meyer and Pienaar 1984; Erata and Chihara 1989).

A markedly different inner plate organization is characteristic of the genus *Cryptomonas*. In thin sections the periplast has a flattened appearance, and the inner plates appear most intimately associated with the PM at their edges (Fig. 7). The inner plates and PM commonly appear separate from one another in *Cryptomonas* although this features may result from shrinkage during fixation for electron microscopy (Kugrens and Lee 1987; Kugrens pers. comm., Hill pers. comm.). In contrast to other genera, the inner plates of *Cryptomonas* are not aligned into rows, but instead exhibit a polygonal (generally hexagonal) arrangement (Hibberd et al. 1971; Faust 1974; Santore 1977, 1984, 1985; Brett and Wetherbee 1986; Kugrens and Lee 1987).

Despite the variation in shape and morphology of inner plates, an extremely close relationship between the IPC and PM is evident in all genera. Freeze-fractures reveal that the PM is organized into discrete regions called domains, which are situated directly above inner plates (Figs. 8 and 9). The domains are densely packed with intra-membrane particles (IMPs), and may possess specialized rows of IMPs in regions where the IPC and PM are strongly attached (Hausmannn and Walz 1979; Brett and Wetherbee 1986; Hill and Wetherbee 1986, 1988; Kugrens and Lee 1987). The location and arrangement of attachment sites varies between genera. In *Cryptomonas*, particles are evident around the entire perimeter of each domain (Fig. 8), while in other genera ordered rows of IMPs are commonly observed along the posterior margins (Fig. 9).

In contrast to the ordered domains, regions of PM above the gaps between inner plates contain fewer, less ordered IMPs. These differences in the IMP organization suggest that the inner plates may act as a cytoskeletal template which directly influences the arrangement of IMPs within the PM.

The cell surface

The use of freeze-fracture/-etch preparation has also enabled examination of cell surface features and their relationship to underlying periplast components. In *Cryptomonas* and *Rhodomonas*, the SPC generally consists of elongate fibrils (or scales in *Rhodomonas stigmatica*) which form a dense mat across most of the cell surface (Brett and Wetherbee 1986, Hill and Wetherbee 1989). The arrangement of the SPC in these cryptomonads does not appear closely linked to the organization of the underlying PM and IPC. In all other cryptomonads discussed in this review, however, an intimate relationship is evident between the SPC, PM and IPC. The SPC is composed of discrete plates situated directly above ordered domains in the PM (e.g., Fig. 10).

The details of surface plates vary markedly between genera, and often provide important criteria for the separation of taxa (Table 1). In *Plagioselmis*, the surface plates are composed of particulate material and granular scales (Fig. 11), those of *Rhinomonas* (Hill and Wetherbee 1988) are composed of rod-like subunits with a triangular arrangement (Figs. 12 and 13), while *Komma, Falcomonas, Chroomonas* (Hill 1991 a), and *Proteomonas sulcata* (haplomorph) (Hill and Wether-

---

Figs. 3–5. Freeze-etch images of cryptomonad cell surfaces. Bars: Figs. 3 and 5, 0.5 μm; Fig. 4, 0.2 μm

Fig. 3. The SPC of *Proteomonas sulcata* (diplomorph), showing a dense mat of elongate fibrils

Fig. 4. Heptagonal scales form the SPC of *Geminigera cryophila*

Fig. 5. Ordered crystalline plates on the cell surface of *Proteomonas sulcata* (haplomorph)

Figs. 6 and **7.** Thin sections through periplast. Bars: Fig. 6, 0.2 μm; Fig. 7, 0.5 μm

Fig. 6. The IPC of *Proteomonas sulcata* consists of discrete anteriorly stepped plates. Ejectisome vesicles (*E*) are located adjacent to the anterior corners of each inner plate

Fig. 7. IPC of *Cryptomonas ovata* has a flattened appearance in T.S. The discrete inner plates (*IPC*) appear intimately associated with the PM at their edges (arrows). Ejectisome vesicles (*E*) associate with the PM in the gaps between plates

Figs. 8 and **9.** Freeze-fracture images of PM. Bars: Fig. 8, 0.5 μm; Fig. 9, 0.2 μm

Fig. 8. Polygonal arrangement of PM domains in *Cryptomonas ovata*. PM domains are densely packed with IMPs, and surrounded by a highly ordered row of particles (arrowheads). Ejectisome vesicles (*E*) are present adjacent to the corners of domains

Fig. 9. A distinct row of IMPs (arrows) defines the posterior margins of PM domains in *Proteomonas sulcata* (haplomorph). Regions of PM between adjacent domains contain fewer IMPs and have a pitted appearance

Table 1. Cryptomonads possessing an IPC of discrete plates. Variations in periplast morphology and arrangement are evident between genera

Organism	Vestibulum: furrow or/ and gullet	IPC type[a]	General shape of plate areas	Attachment sites between IPC and PM	Arrangement of plate areas	Modifications in mid-ventral region	SPC type[b]	Component of SPC	Ordered plate borders	Specialised features of cell posterior
Chroomonas	gullet	A	± rectangular	posterior of PM domain	longitudinal rows	nil	A	hexagonally packed subunit	present	raphe
Komma	gullet	A	± hexagonal	posterior of PM domain	long. rows	*nil*	A		present	tail-plate
Rhinomonas	gullet	A	± hexagonal	posterior of PM domain	long. rows	plate areas reduced in size	A	triangular packing, rod-like subunits	present	raphe-like structure
Proteomonas sulcata (haplomorph)	furrow	A	± hexagonal (rounded anterior)	posterior of PM domain	long. rows	no plate areas	A	hexag. packed subunits	present	MVB
Falcomonas	furrow	A	± hexagonal	nil	long. rows	no plate areas	A	hexag. packed subunits	absent	MVB
Plagioselmis	furrow	A	± hexagonal	nil	long. rows	no plate areas	A	granules and scales	present	MVB
Rhodomonas	furrow and gullet	A	± rectangular	posterior of PM domain	long. rows	plate areas reduced i.s.	B	fibrils (scales in *R. stigm.*)	absent	plate areas often absent
Cryptomonas	furrow and gullet	B	polygonal (rounded corners)	edges of PM domain	polygonal	plate areas reduced i.s.	B	fibrils	absent	plate areas small and irregular in shape

Variations in the shape of plate areas may occur during preparation of cells for EM (particularly SEM). Santore (1977) cautioned against sole use of this feature in critical taxonomic determinations

[a] *A* Discrete plates closely appressed to PM; *B* discrete plates attached to PM at edges

[b] *A* Organised surface plates; *B* no surface plates

bee 1986) possess highly ordered crystalline plates (Figs. 14–17). Crystalline plates are composed of minute subunits precisely arranged into ordered lattices. Regions of the cell surface between adjacent plates have a markedly different appearance; they contain particulate material that may be randomly arranged (Fig. 14), or aligned into distinct raised borders (Figs. 10 and 14–17). Close examination of these areas reveals that the particulate material is similar in size to (and may display continuity with) the lattice subunits (Figs. 16 and 17).

Recent immunological studies on *Komma caudata* suggest that subunits which comprise the lattices and borders of the SPC in this organism are high molecular weight glycoproteins (Perasso et al. 1994). Monoclonal antibodies selected for surface labelling recognize both the crystalline lattices and plate borders, with most intense labelling occurring in the border regions (e.g., Figs. 50–53). Similar observations have also been reported for the Volvocalean alga *Lobomonas piriformis*, which possesses a layered cell wall overlain by crystalline surface plates surrounded by amorphous boundaries (Roberts et al. 1981, Shaw and Hills 1982). Studies on *L. piriformis* indicate that subunits at plate edges are the same as those within the crystalline lattice, and suggest that conformational changes or biochemical modification of edge subunits is necessary for incorporation into lattices. The intense labelling observed at the plate borders in both *L. periformis* and *K. caudata* suggests that the epitope recognized by the surface antibody is most accessible when subunits are in the border conformation (reviewed in Perasso et al. in prep.).

In the cryptomonads, variations in the arrangement of the border and lattice subunits appear closely associated with the organization of the underlying IPC and PM. Lattices are always located directly above ordered domains and inner plates, whereas the borders are positioned above gaps in the IPC (Fig. 10). These features suggest that alignment of the subunits into the crystalline lattices may be directly influenced by underlying IMPs within PM domains. The domains (and IPC) may act to bind or induce conformational changes in these molecules that will facilitate their consolidation into the ordered lattice arrangement.

Arrangement of plate areas across cryptomonad cells

In all the cryptomonads examined in this review, the inner plates, PM domains and associated surface structures from discrete regions termed plate areas (Gantt 1971). The plate areas are present in most regions of the cell periphery but do not extend into the vestibulum, furrow or gullet. These regions are bounded only by PM, which contains few IMPs and has a disordered appearance in freeze-fracture images (Figs. 18 and 19). Elsewhere, however, plate areas form a highly ordered system.

Studies using SEM and freeze-fracture/-etch have allowed detailed investigation of periplast arrangement and reveal considerable variation in the size (and to some extent shape) of these plate areas across cryptomonad cells (Brett and Wetherbee in prep.). In all cryptomonads examined using these techniques, plate areas appear largest in the equatorial regions, and are generally reduced in size as cells taper toward the anterior and posterior (Figs. 18–21). In addition to these variations in size, the arrangement of plate areas across the ventral surface is often highly specialized. The periplast is commonly separated along the mid-ventral line, with plate areas adjacent to this region reduced in size and modified in shape (Figs. 18, 22, and 23). Although this unusual arrangement is most conspicuous in cryptomonads which possess a furrow, separation of the periplast along the entire mid-ventral line is evident in all genera discussed here except *Komma* and *Chroomonas*. Further modifications in the arrangement of plate areas are also observed in the posterior of cryptomonad cells. The periplast may be absent from this region, or alternately may terminate adjacent to specialized features including the raphe (Gantt 1971, Hill 1991 a), tail plate (Hill 1991 a), or mid-ventral band (Hill and Wetherbee 1986, 1989; Hill 1991 a).

Changes in periplast arrangement throughout the cell cycle

Recent studies have directed attention to changes in periplast arrangement and organization throughout the cell cycle (Brett and Wetherbee in prep.). These reports reveal that substantial development of the periplast occurs during cytokinesis, and also following division as cells enlarge and mature. Cell division in the cryptomonads (Perasso et al. 1992, 1993) involves a unique process termed pole reversal. During cytokinesis the tail regions of daughter cells develop from the anterior of the parental cell, necessitating complete realignment of the periplast. Although slight variations occur between cryptomonad genera, the major features of this unusual mode of cell division are similar throughout the group, and are described here for *K. caudata*.

At the onset of division, flagella replication occurs in the vestibulum, and lateral expansion of cells is ap-

parent (Figs. 24 and 25). The periplast separates along the mid-ventral line progressing from the vestibulum toward the cell posterior. The edges of the periplast exposed during this process form specialized regions, termed anamorphic zones, which undergo developmental changes both during and after cytokinesis. As the ventral surface divides, these regions, as well as additional anamorphic zones located around the vestibular margins, expand and realign (Figs. 26–28). Distinct pointed structures form where the anamorphic zones converge, and eventually develop into the tail regions of daughter cells. The dorsal surface then divides, the forming tail regions migrate laterally (Figs. 29–31) and rotation of cell halves relative to one

---

Fig. 10. Freeze-fracture/-etch of *Proteomonas sulcata* (haplomorph). The cell surface consists of ordered crystalline plates, surrounded by distinct raised borders (*b*). The plates are located directly above PM domains, while borders are located above less ordered regions of PM (arrows); 0.5 μm

Figs. 11–17. Freeze-etch images of cryptomonad cell surfaces. Bars: Figs. 11 and 13–15, 0.5 μm; Fig. 12, 0.2 μm; Figs. 16 and 17, 0.1 μm

Fig. 11. The surface plates of *Plagioselmis prolonga* are covered in particulate material and granular scales (*s*). Plates are surrounded by raised borders (*b*)

Fig. 12. Surface plates of *Rhinomonas pauca* consisting of rod-like subunits with a triangular arrangement. Border regions (*b*) are composed of elongate subunits

Fig. 13. Arrangement of surface plates in *Rhinomonas pauca*

Fig. 14. SPC of *Falcomonas daucoides*. The crystalline plates are composed of minute subunits. Border regions (*b*) contain disordered particulate material

Fig. 15. The crystalline plates of *Proteomonas sulcata* (haplomorph) are surrounded by distinct raised borders (*b*). Scales are also evident on plate surfaces (*s*)

Fig. 16. Detail of crystalline plate of *Proteomonas sulcata* (haplomorph) showing ordered arrangement of subunits. Border (*b*) subunits may occasionally appear continuous with those of the lattice (arrow)

Fig. 17. SPC of *Komma caudata* showing continuity between lattice and border (*b*) subunits

Figs. 18–21. Freeze-fracture images (PF) of *Proteomonas sulcata* (haplomorph). Bars: Figs. 18 and 21, 0.5 μm; Fig. 19, 0.2 μm; Fig. 20, 1 μm

Fig. 18. Ventral surface of cell, showing reduced PM domains adjacent to the vestibulum (*V*) and furrow (*Fu*). A mid-ventral band (*MV*) extends posteriorly from the furrow

Fig. 19. Small PM domains (arrows) at the margins of the vestibulum (*V*)

Fig. 20. The MV passes along the mid-ventral line to the cell posterior. Regions of PM adjacent to this structure contain few, randomly arranged IMPs (stars). PM domains are smallest at the edges of the periplast (arrow)

Fig. 21. Small PM domains (arrows) at the margins of the periplast adjacent to the mid-ventral line in the cell posterior

Figs. 22 and **23.** Freeze-fracture images (PF) of *Rhinomonas pauca*. Bars: 0.5 μm

Fig. 22. Ventral surface showing reduced size of PM domains (arrows) adjacent to the mid-ventral line. This specialization passes from the vestibulum (*V*) to cell posterior

Fig. 23. Small PM domains along mid-ventral line (line) appear less rigidly organized than adjacent domains

Figs. 24–32. SEM images of *Komma caudata* during cell division. Bars: 2 μm

Figs. 24 and **25.** Periplast separates along the mid-ventral line at onset of division. Lateral expansion of cells occurs

Figs. 26–28. Mid-ventral (*mva*) and vestibular (*va*) anamorphic zones expand and realign. Pointed tail regions form where the anamorphic zones converge (large arrows). Periplast develops a flattened appearance

Figs. 29–31. Forming tail regions separate laterally and dorsal surface divides. Anamorphic zones align along the mid-ventral line of forming daughter cells (arrowheads)

Fig. 32. Cell halves rotate to facilitate separation

Figs. 33–35. SEM images of *Komma caudata* following cell division. Bars: 2 μm

Fig. 33. Periplast of daughter cells is highly ordered but divided along the mid-ventral line. Small plate areas are evident adjacent to this region

Fig. 34. As cells enlarge the periplast becomes continuous across the ventral surface

Fig. 35. Mature cell showing well defined vestibulum, and increase in number of plate areas comprising the periplast

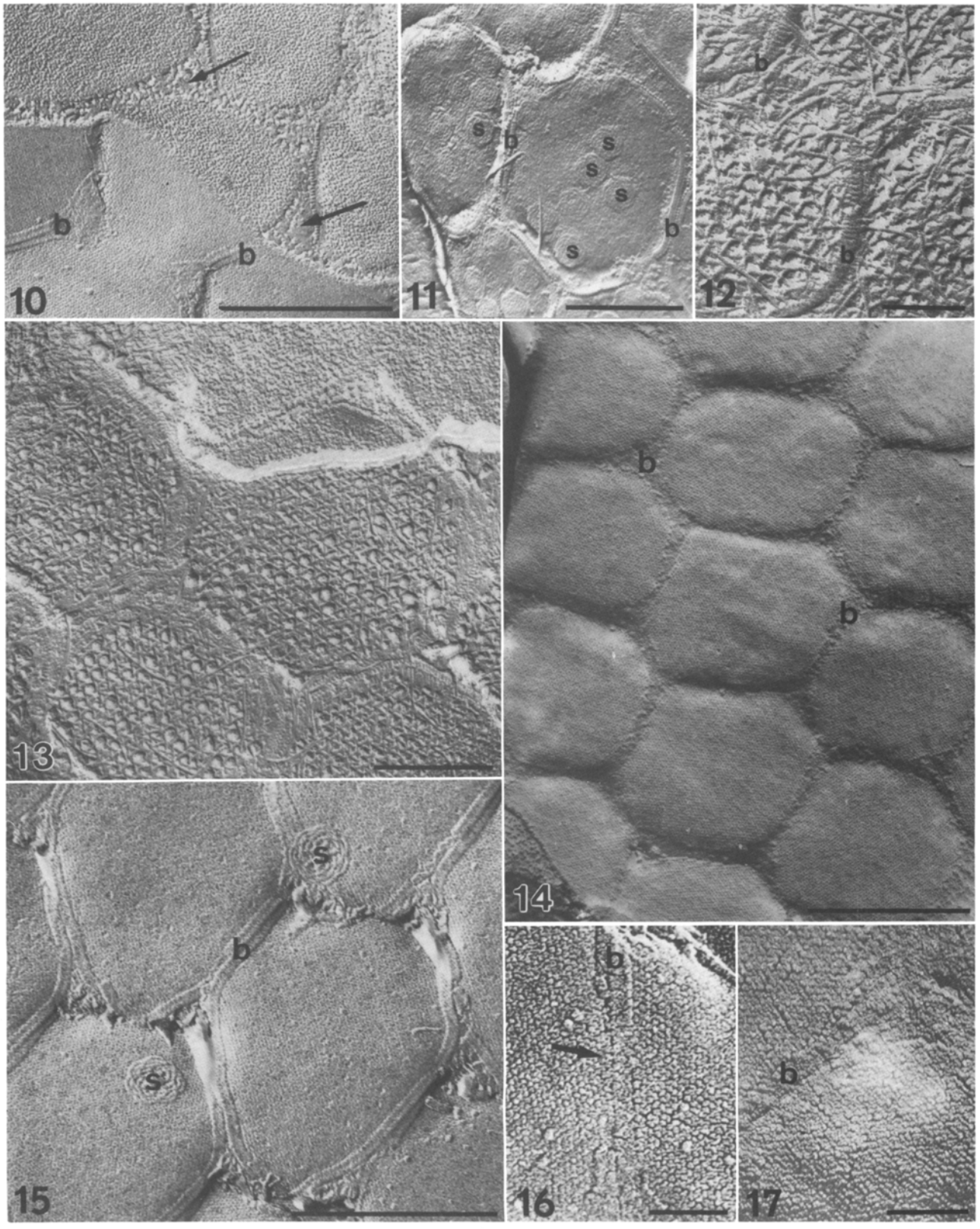
10
b
b
11
s
b
s
s
s
s
b
12
b
b
13
14
b
b
15
s
b
s
16
b
17
b

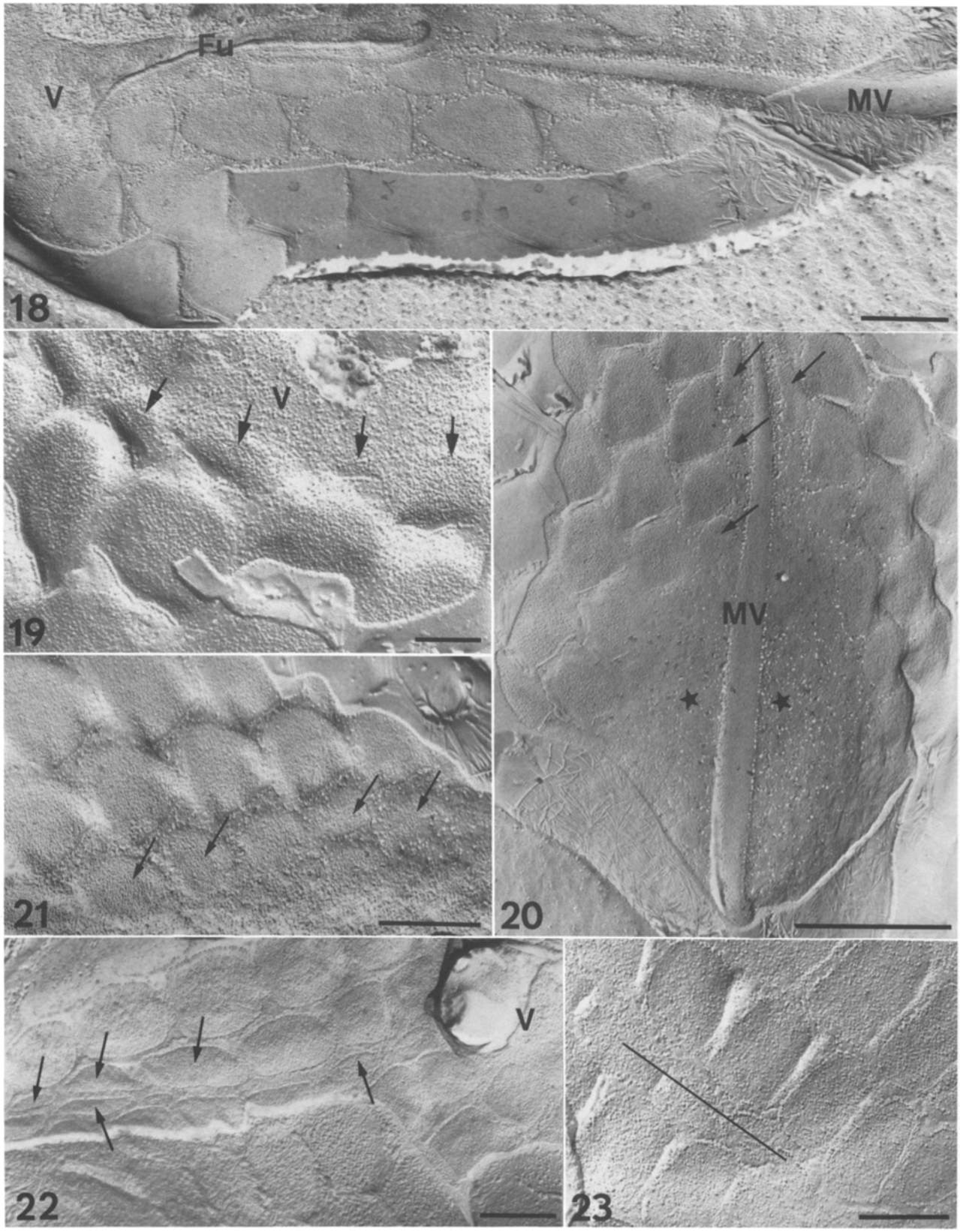
Fu
V
MV
18
V
19
MV
20
21
V
22
23

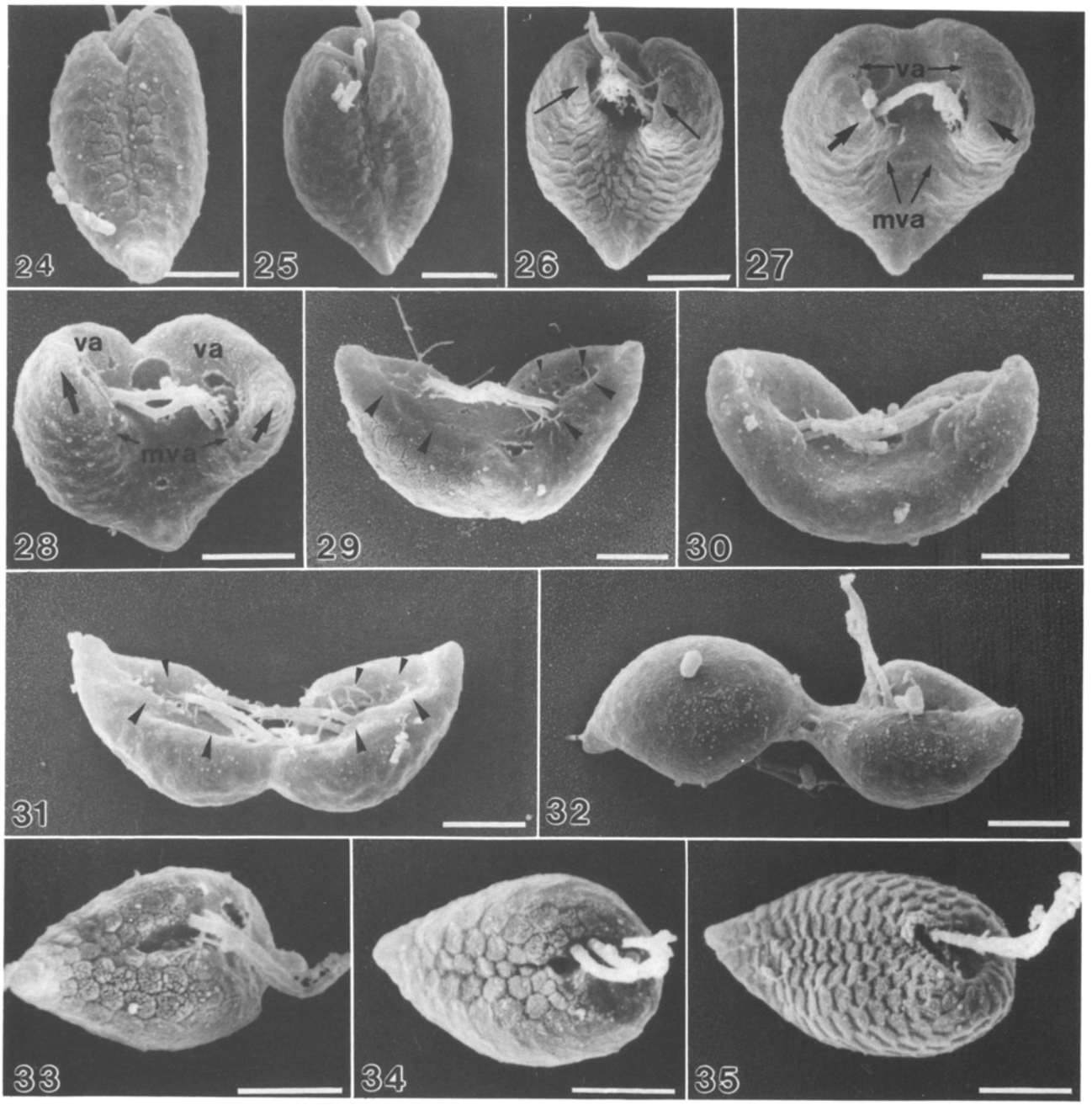
24
25
26
va
mva
27
va
va
mva
28
29
30
31
32
33
34
35

another facilitates separation (Fig. 32). Further realignment of the anamorphic zones occurs, and these eventually position on either side of the mid-ventral line of developing daughter cells (Figs. 32 and 33).

The unusual mode of cell division in the cryptomonads, involving reorientation of daughter cells relative to the parental cell, necessitates major changes in the periplast in many cryptomonads (Brett and Wetherbee 1994 a). In cells with anteriorly stepped plate areas, the periplast persists, but develops a flattened appearance during cell division (Figs. 27–32). The plate areas remain precisely aligned throughout this process, and after cytokinesis adopt a polarity consistent with the newly formed daughter cell. Although the process of periplast reorientation is not fully understood, detailed examination of cells using thin sections and freeze-fracture/-etch suggests that realignment may be facilitated by relocation of the attachment sites between inner plates and the PM (Brett and Wetherbee in prep.).

Following cell division, daughter cells are substantially smaller than their parental counterparts, the vestibular margins are indistinct and the periplast is always divided along the mid-ventral line (Fig. 33). As cells enlarge and mature the vestibulum/furrow/gullet complex becomes more clearly defined, and changes in periplast organization occur. In *Komma* (Figs. 34 and 35) and *Chroomonas* the periplast becomes continuous across the ventral surface as the gullet develops, although in all other organisms the periplast remains separated along the mid-ventral line throughout the cell cycle (Figs. 36–39).

The elongation and lateral expansion of cells that occurs after division is associated with an increase in the number of plate areas comprising the periplast (Figs. 33–39). The periplast remains precisely aligned throughout this process, suggesting that growth occurs in an orderly manner by addition of new plate areas to anamorphic zones (Brett and Wetherbee in prep.). In most genera elongation results from addition of new plate areas to anamorphic zones around the vestibulum and in the posterior, while lateral expansion is facilitated by growth and addition from the mid-ventral line (Figs. 36–39). Growth from these anamorphic zones appears to enable highly ordered expansion of cryptomonads throughout the entire cell cycle. The absence of mid-ventral specializations in *Komma* (Figs. 34 and 35) suggests, however, that lateral expansion in this genus may occur by the enlargement of existing plates in the ventral regions of the cell.

Formation and development of the inner plates

The general changes in the arrangement of plate areas revealed in the SEM studies provided a basis for more detailed investigation of periplast development. Subsequent work (which indirectly examined the formation and growth of the inner periplast plates using freeze fracture images) revealed variations in the size, organization and alignment of PM domains within anamorphic zones (Brett and Wetherbee in prep.). Despite differences in the morphology of the inner plates between genera, similar features were observed in all cryptomonads examined.

Figs. 36–39. SEM images of *Proteomonas sulcata* (haplomorph) following cell division. Bars: 1 μm

Fig. 36. Immediately after cell division vestibular margins and furrow are not clearly defined. Periplast is highly ordered but has a flattened appearance

Fig. 37. As cells enlarge the anteriorly stepped periplast polarity becomes evident

Fig. 38. An increase in number of plate areas comprising the periplast occurs as cells enlarge. Periplast remains highly ordered as growth occurs

Fig. 39. The periplast remains divided along the mid-ventral line throughout the cell cycle. Growth of the periplast occurs by addition of new plate areas from anamorphic zones around vestibulum, mid-ventral line and cell posterior (arrowheads)

Figs. 40 and **41.** Freeze-fracture images (PF) of *Cryptomonas ovata*. Bars: 0.5 μm

Fig. 40. PM domains around anamorphic zones are smaller and less rigidly ordered than in other regions of the cell

Fig. 41. Gradation in the size of PM domains adjacent to vestibulum (*V*)

Figs. 42 and **43.** Freeze-fracture images (EF) of *Rhodomonas baltica*. Bars: 0.2 μm

Fig. 42. Vestibular anamorphic zone at onset of division. PM domains show variations in size and irregular alignment

Fig. 43. Mid-ventral line at onset of division. Periplast is distinctly divided in this region and small PM domains are located at edges of the anamorphic zone (arrows)

The PM domains within anamorphic zones range over a continuum from minute accumulations or circular aggregates of IMPs to larger, more rigidly ordered regions densely packed with IMPs and possessing specialized attachment sites. Although most conspicuous in dividing and newly formed cells (Figs. 40–43), similar variations are evident adjacent to anamorphic zones throughout the cell cycle (Figs. 18–23). The distinct

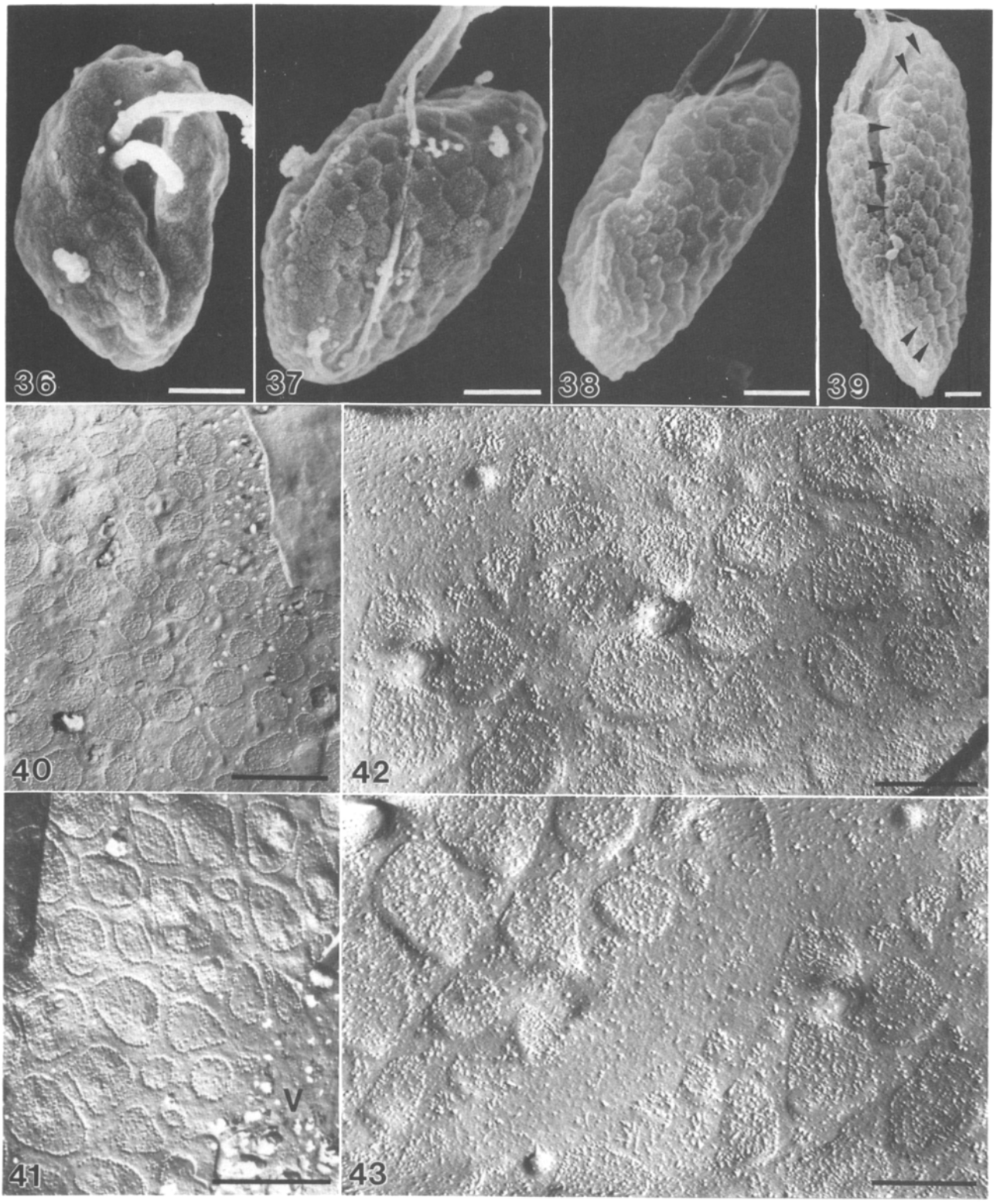

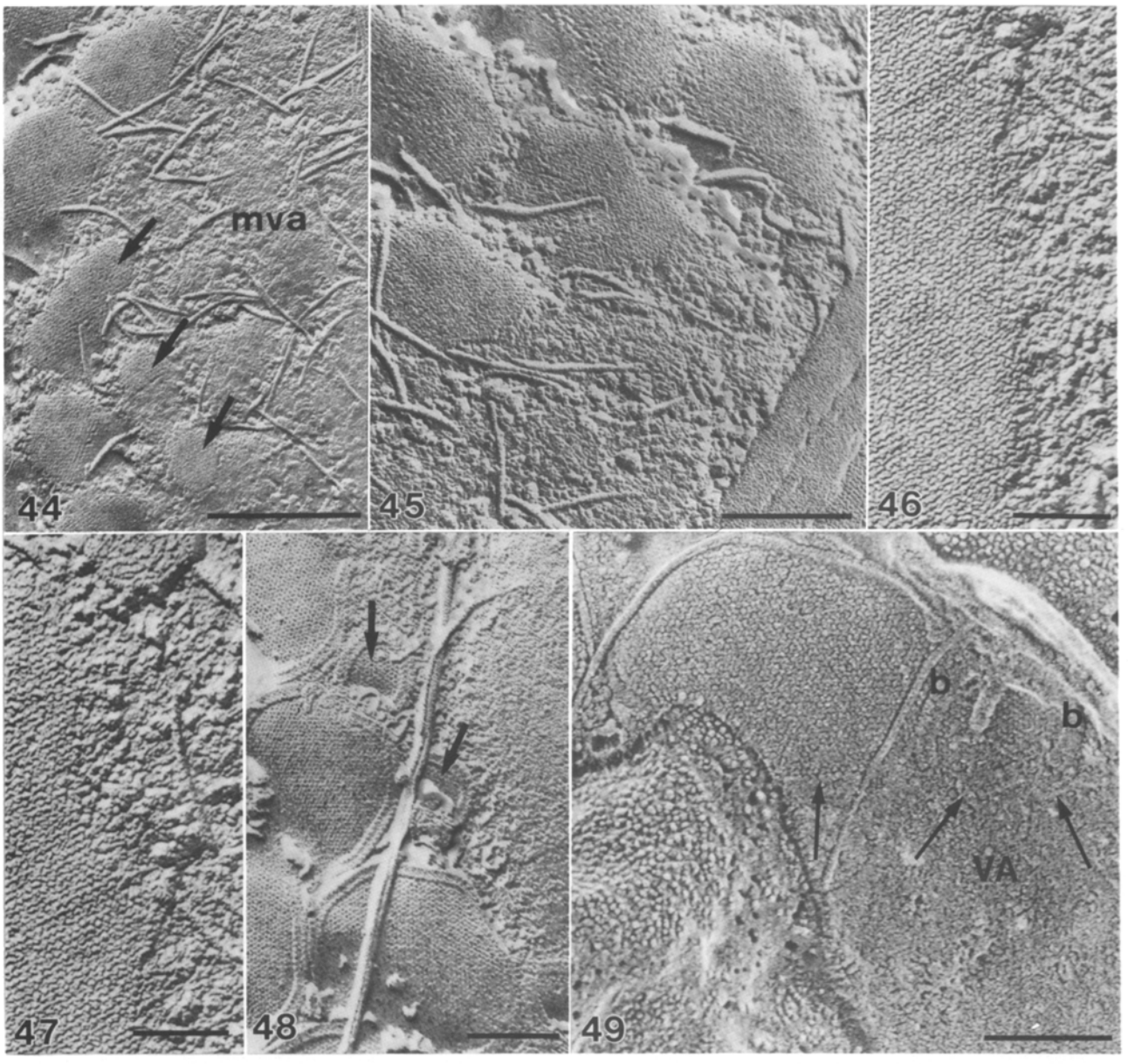

Figs. 44–47. Freeze-etch images around anamorphic zones in *Falcomonas daucoides*. Bars: Fig. 44, 0.5 µm; Fig. 45, 0.2 µm; Figs. 46 and 47, 0.1 µm

Fig. 44. Surface plates adjacent to the mid-ventral anamorphic zone (*mva*) are reduced in size (arrows). Surrounding regions of cell surface contain disordered particles and elongate fibrils

Fig. 45. Particulate material adjacent to the periplast may align into loose aggregates. The plate edges are often indistinct, and closely associated with this material

Figs. 46 and **47.** Surrounding surface particles are similar in size, and often appear continuous with subunits of the crystalline surface lattices

Figs. 48 and **49.** Freeze-etch images around anamorphic zones in *Proteomonas sulcata* (haplomorph). Bars: 0.2 µm

Fig. 48. Vestibular anamorphic zone. Surface plates are reduced in size (arrows), but are surrounded by distinct raised borders

Fig. 49. Vestibular anamorphic zone (*VA*) in dividing cell. The lattice subunits, borders subunits (*b*) and less ordered particulate material may occasionally appear continuous during rapid periplast development (arrows)

gradation in the size of domains within these regions indicates that growth of the periplast does not occur by addition of large, fully formed inner plates at the edges of the IPC. The features observed suggest, instead, that the inner plates form de novo and undergo considerable enlargement within these specialized anamorphic zones. Variations in the spacing and arrangement of PM domains in developing cells (Figs. 40, 42, and 43) imply that the inner plates develop independently, and are capable of some movement relative to one another as they align within the highly ordered periplast.

Development of crystalline surface plates

The intimate relationship between IPC, PM and SPC in the cryptomonads suggests that the development of crystalline surface plates may be closely linked to the formation and growth of the inner plates within anamorphic zones. The unique SPC of *Falcomonas daucoides*, comprising crystalline surface plates which lack distinct borders (Hill 1991 a), provides a model system for investigation of features associated with lattice development (Brett and Wetherbee in prep.). Examination of this organism reveals that surface plates within anamorphic zones are commonly reduced in size, and surrounding areas of the cell surface are covered with disordered particulate material (Figs. 44 and 45). The surface particles are similar in size to lattice subunits, and may be aligned into loose aggregates or closely associated with the edges of periplast plates (Figs. 45–47). Plate margins are often indistinct and surface particles adjacent to these regions may appear continuous with, and are often indistinguishable from, lattice subunits.

The close relationship between the particulate material and lattice subunits suggests that development of the crystalline surface may occur by accumulation and incorporation of less ordered precursors from surrounding regions of the cell surface. After formation of these crystalline plates, enlargement and growth appears facilitated by addition of subunits to the lattice edges. Detailed studies of bacteria (for reviews, see Sleytr and Messner 1983, Messner and Sleytr 1992) and *L. piriformis* (Roberts et al. 1981, Shaw and Hills 1982) describe a similar mode of lattice development and suggest that conformational changes occur to precursor molecules during addition. As stated above, the close spatial relationship between the organization of the IPC, PM and SPC in the cryptomonads suggests that the formation and enlargement of surface plates may be intimately associated with developmental changes in the IPC and PM. Growth of the inner plates and related expansion of PM domains, may induce changes in the precursor molecules which enable incorporation into the highly ordered lattice.

Although the relatively simple arrangement of the SPC in *F. daucoides* provides an ideal system for examination of lattice assembly, the crystalline surface plates in other genera are generally surrounded by distinct raised borders (Figs. 48 and 49) (Hill and Wetherbee 1986, Hill 1991 a). Consequently, growth of these lattices during self-assembly does not appear to occur by direct addition of disordered precursors from surrounding regions of the cell surface. The continuity between borders and lattices in these organisms (Figs. 16, 17, and 49) suggests, instead, that subunits may be rearranged. For example, subunits previously within a border may subsequently become incorporated into the highly ordered surface plates during development (Brett and Wetherbee in prep.). The close relationship between the organization of the SPC and underlying periplast components indicates that incorporation of border subunits into the lattices during self-assembly may be closely associated with the growth of inner plates and PM domains.

The immunological work of Perasso et al. (in prep.) also suggests similarities between the components comprising the lattices, borders and less ordered regions of the cell surface. These studies indicate that the subunits which form the SPC are produced in the Golgi apparatus and secreted through the endomembrane system for deployment at the edges of the periplast (Figs. 50–53). Examination of *K. caudata* through the cell cycle reveals that deposition of these macromolecules occurs predominantly within anamorphic zones, where the majority of lattice formation occurs.

Conclusions

The complexity of the cryptomonad periplast has necessitated use of a wide range of techniques to accurately determine morphology of the IPC, PM and SPC. Although general features of periplast structure and arrangement may be determined using thin sections and SEM, the use of freeze-fracture/-etch has greatly enhanced the understanding of this unique organelle. Studies incorporating these techniques reveal considerable diversity throughout the Cryptophyceae and provide important characters for taxonomic distinctions within the group. The detailed information about PM and surface microarchitecture available from these

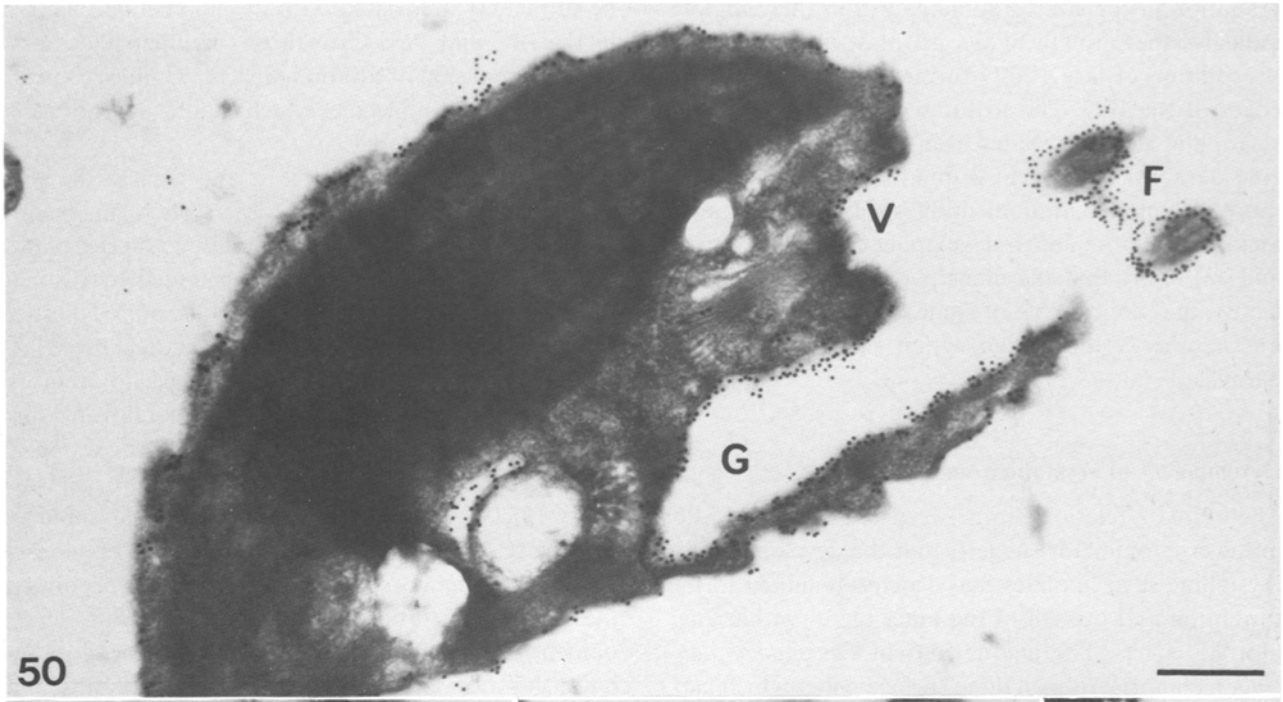
V
F
G
50

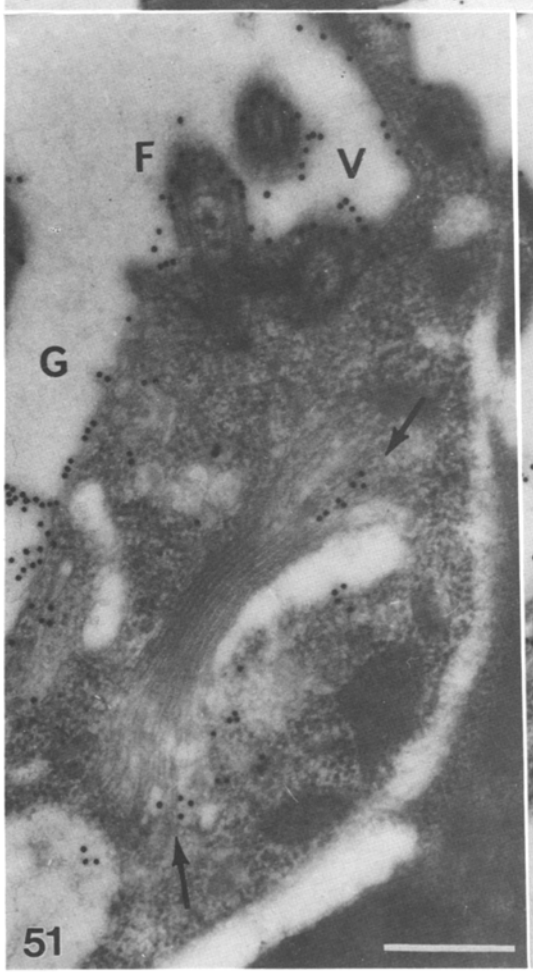
F
V
G
51

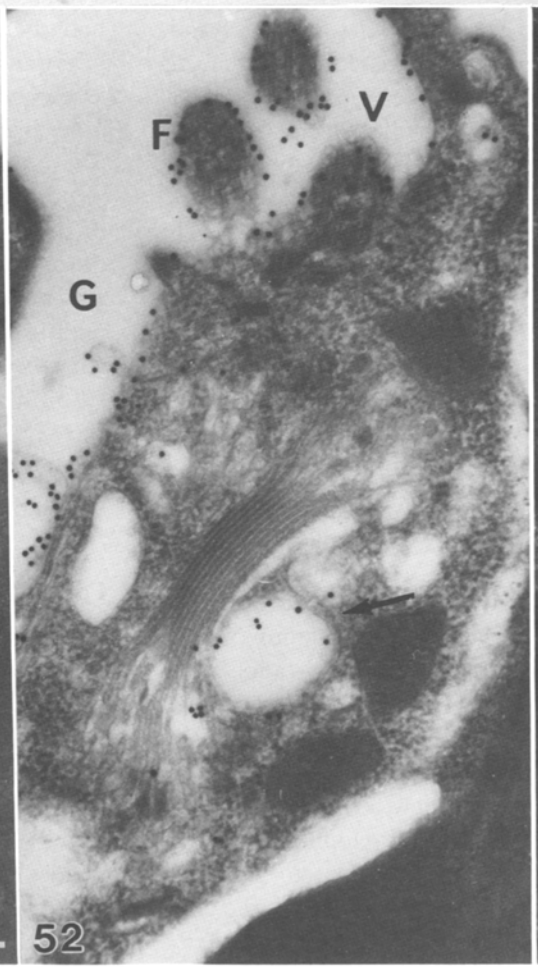
F
V
G
52

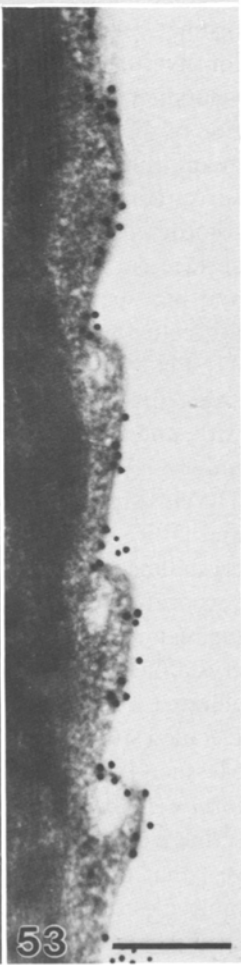
53

reports has also enabled examination of the complex relationships between components comprising the periplast.

The cells discussed in this review all possess an IPC of discrete plates, and have proven ideal systems for investigation of the association between IPC, PM, and SPC. In all these organisms the PM is ordered into discrete domains which are situated directly above the inner periplast plates. In contrast, regions of the PM not supported by the IPC generally contain fewer IMPs and appear less ordered. The IPC-PM association suggests that the inner plates are cytoskeletal, and may influence the arrangement of IMPs within the PM. Organization of the crystalline surface plates found in many cryptomonad genera also appears closely associated with that of the underlying components. The location of these plates directly above ordered PM domains suggests that the PM, and ultimately the IPC, may influence the alignment of subunits within surface lattices.

Development of both the IPC and SPC occurs from specialized anamorphic zones throughout the cell cycle. Unlike the wall components of many microalgal groups, fully formed inner and surface plates are not pre-packaged within cytoplasmic vesicles for later addition to the periplast. Instead the inner periplast plates appear to form de novo and undergo considerable enlargement within anamorphic zones. Growth of the crystalline surface lattices, which occurs by addition and incorporation of less ordered precursors from surrounding surface areas, may be closely associated with this process. The intimate relationship between IPC, PM, and SPC suggests that growth of inner plates and PM domains may result in modifications which enable incorporation of precursor molecules into the highly organized surface lattices. The precise mode of formation may be more fully understood as further details of periplast chemistry are revealed.

Acknowledgements

RW thanks the Australian Research Council for financial assistance. SJB and LP were supported by Commonwealth Postgraduate Scholarships, the University of Melbourne. We thank Dr. Paul Kugrens for Fig. 1 and Dr. David R. A. Hill for valuable discussions and for reviewing the manuscript.

References

Antia NJ, Kalley JP, McDonald J, Bisalputra T (1973) Ultrastructure of the marine cryptomonad *Chroomonas salina* cultured under conditions of photoautotrophy and glycerol-heterotrophy. J Protozool 20: 377–385

Brett SJ, Wetherbee R (1986) A comparative study of periplast structure in *Cryptomonas cryophila* and *C. ovata* (Cryptophyceae). Protoplasma 131: 23–31

Dodge JD (1969) The ultrastructure of *Chroomonas mesostigmatica* Butcher (Cryptophyceae). Arch Microbiol 69: 266–280

Erata M, Chihara M (1989) Re-examination of *Pyrenomonas* and *Rhodomonas* (Class Cryptophyceae) through ultrastructural survey of red pigmented cryptomonads. Bot Mag Tokyo 102: 429–443

Faust MA (1974) Structure of the periplast of *Cryptomonas ovata* var. *palustris*. J Phycol 10: 121–124

Gantt E (1971) Micromorphology of the periplast of *Chroomonas* sp. (Cryptophyceae). J Phycol 7: 177–184

Grim JN, Staehelin LA (1984) The ejectisomes of the flagellate *Chilomonas paramecium*: visualization by freeze-fracture and isolation techniques. J Protozool 31: 259–267

Hausmann K, Walz B (1979) Periplaststruktur und Organisation der Plasmamembrane von *Rhodomonas* spec. (Cryptophyceae). Protoplasma 101: 349–354

Hibberd DJ, Greenwood AD, Griffiths HB (1971) Observations on the ultrastructure of the flagella and periplast in the Cryptophyceae. Br Phycol J 6: 61–72

Hill DRA (1991 a) *Chroomonas* and other blue-green cryptomonads. J Phycol 27: 133–145

– (1991 b) A revised circumscription of *Cryptomonas* (Cryptophyceae) based on examination of Australian strains. Phycologia 30: 179–188

– Wetherbee R (1986) *Proteomonas sulcata* gen. et sp.nov. (Cryptophyceae), a cryptomonad with two morphologically distinct and alternating forms. Phycologia 25: 521–543

– – (1988) The structure and taxonomy of *Rhinomonas pauca* gen. et sp.nov. (Cryptophyceae). Phycologia 27: 355–365

– – (1989) A reappraisal of the genus *Rhodomonas* (Cryptophyceae). Can J Bot 28: 143–158

– – (1990) *Guillardia theta* gen. et sep.nov. (Cryptophyceae). Can J Bot 68: 1873–1876

Klaveness D (1981) *Rhodomonas lacustris* (Pascher & Ruttner) Javornicky (Cryptomonadida): ultrastructure of the vegetative cell. J Protozool 28: 83–90

Figs. 50–53. MAb immunogold labelling of *Komma caudata*. Bars: Figs. 50–52, 1 μm; Fig. 53, 0.5 μm

Fig. 50. Labelling of an interphase cell, labelling is observed over the entire surface, most obvious at the surface plate edges, and also over the vestibular (*V*), gullet (*G*), and flagellar (*F*) surfaces

Figs. 51 and **52.** Labelling of non-consecutive serial sections through a prophase cell, showing labelling about the GA and vesicles associated with the GA (arrows)

Fig. 53. High magnification of labelling of the periplast

Klaveness D (1985) Classical and modern criteria for determining species of Cryptophyceae. Bull Plankton Soc Jap 32: 111–123

Kugrens P, Lee RE, Andersen RA (1986) Cell form and surface patterns in *Chroomonas* and *Cryptomonas* cells (Cryptophyta) as revealed by scanning electron microscopy. J Phycol 22: 512–522

Kugrens P, Lee RE (1987) An ultrastructural survey of cryptomonad periplast using quick-freezing freeze fracture techniques. J Phycol 23: 365–376

– – (1991) Organization of cryptomonads. In: Patterson DJ, Larsen J (eds) The biology of free-living heterotrophic flagellates. Clarendon Press, Oxford, pp 219–233

Lucas IAN (1970) Observations on the fine structure of the Cryptophyceae. 1. The genus *Cryptomonas*. J Phycol 6: 30–38

Messner P, Sleytr UB (1992) Crystalline bacterial cell-surface layers. Adv Microbiol Physiol 33: 213–275

Meyer SR, Pienaar RN (1984) The microanatomy of *Chroomonas africana* sp.nov. (Cryptophyceae). S Afr Tydskr Plank 3: 306–319

Mnawar M, Bistricki T (1979) Scanning electron microscopy of some nanoplankton cryptomonads. Scanning Electron Microsc 3: 247–252

Perasso L, Hill DRA, Wetherbee R (1992) Transformation and development of the flagellar apparatus of *Cryptomonas ovata* (Cryptophyceae) during cell division. Protoplasma 170: 53–67

– Brett SJ, Wetherbee R (1993) Pole reversal during cytokinesis in the Cryptophyceae. Protoplasma 174: 19–24

Roberts K, Shaw PJ, Hills GJ (1981) High-resolution electron microscopy of glycoproteins: the crystalline cell wall of *Lobomonas*. J Cell Sci 51: 295–321

Santore UJ (1977) Scanning electron microscopy and comparative micromorphology of the periplast of *Hemiselmis rufescens*, *Chroomonas* sp., *Chroomonas salina* and members of the genus *Cryptomonas* (Cryptophyceae). Br Phycol J 12: 255–270

– (1982) Comparative ultrastructure of two members of the Cryptophyceae assigned to the genus *Chroomonas* – with comments on their taxonomy. Arch Protistenk 125: 5–29

– (1984) Some aspects of taxonomy in the Cryptophyceae. New Phytol 98: 627–646

– (1985) A cytological survey of the genus *Cryptomonas* (Cryptophyceae) with comments on its taxonomy. Arch Protistenk 130: 1–52

– (1986) The ultrastructure of *Phyrenomonas heteromorpha* comb. nov. (Cryptophyceae). Bot Mar 29: 75–82

– (1987) A cytological survey of the genus *Chroomonas* – with comments on the taxonomy of this natural group of the Cryptophyceae. Arch Protistenk 134: 83–114

Shaw PJ, Hills GJ (1982) Three-dimensional structure of a cell wall glycoprotein. J Mol Biol 162: 459–471

Sleytr UB, Messner P (1983) Crystalline surface layers on bacteria. Annu Rev Microbiol 37: 311–339

Wetherbee R, Hill DRA, McFadden GI (1986) Periplast structure of the cryptomonad flagellate *Hemiselmis brunnescens*. Protoplasma 131: 11–22

– – Brett SJ (1987) The structure of the periplast components and their association with plasma membrane in a cryptomonad flagellate. Can J Bot 65: 1019–1026